



HAL
open science

Pickering nano-emulsions stabilized by Eudragit RL100 nanoparticles as oral drug delivery system for poorly soluble drugs

Sidy Mouhamed Dieng, Ziad Omran, Nicolas Anton, Oumar Thioune, Alphonse Rodrigue Djiboune, Papa Mady Sy, Nadia Messaddeq, Saïd Ennahar, Mounibé Diarra, Thierry Vandamme

► To cite this version:

Sidy Mouhamed Dieng, Ziad Omran, Nicolas Anton, Oumar Thioune, Alphonse Rodrigue Djiboune, et al.. Pickering nano-emulsions stabilized by Eudragit RL100 nanoparticles as oral drug delivery system for poorly soluble drugs. *Colloids and Surfaces B: Biointerfaces*, 2020, 191, pp.111010. 10.1016/j.colsurfb.2020.111010 . hal-02866107

HAL Id: hal-02866107

<https://hal.science/hal-02866107v1>

Submitted on 20 May 2022

HAL is a multi-disciplinary open access archive for the deposit and dissemination of scientific research documents, whether they are published or not. The documents may come from teaching and research institutions in France or abroad, or from public or private research centers.

L'archive ouverte pluridisciplinaire **HAL**, est destinée au dépôt et à la diffusion de documents scientifiques de niveau recherche, publiés ou non, émanant des établissements d'enseignement et de recherche français ou étrangers, des laboratoires publics ou privés.



Distributed under a Creative Commons Attribution - NonCommercial 4.0 International License

Pickering nano-emulsions stabilized by Eudragit RL100 nanoparticles as oral drug delivery system for poorly soluble drugs

Sidy Mouhamed Dieng,^{1,2,3,#,*} Ziad Omran,^{4,#,*} Nicolas Anton,¹ Oumar Thioune,² Alphonse Rodrigue Djiboune,² Papa Mady Sy,² Nadia Messaddeq,⁵ Said Ennahar,⁶ Mounibé Diarra,² Thierry Vandamme^{1,*}

1 Université de Strasbourg, CNRS, CAMB UMR 7199, F-67000 Strasbourg, France

2 Université cheikh Anta Diop de Dakar, laboratoire de pharmacie galénique, Faculté de Médecine, de Pharmacie, laboratoire de physique et biophysique pharmaceutique, Faculté de Médecine, de Pharmacie et d'Odontologie, BP : 5005, Dakar Fann, Sénégal

3 Université de Thiès, laboratoire de pharmacie galénique, UFR santé de Thiès, Thies, Sénégal Cité Malick SY BP 967 Thiès

4 Department of Pharmaceutical Chemistry, College of Pharmacy, Umm AlQura University, 21955 Makkah, Kingdom of Saudi Arabia.

5 Université de Strasbourg, IGBMC, Inserm U1258, CNRS UMR7104, F-67000 Strasbourg, France

6 Université de Strasbourg, IPHC, UMR 7178, IPHC-DSA, CNRS, F-67400 Illkirch-Graffenstaden, France

these authors contributed equally

* To whom correspondence should be addressed:

- Dr Sidy Mouhamed Dieng, Université Cheikh Anta Diop de Dakar et Université de Thiès, laboratoire de pharmacie galénique, industriel et biopharmacie, Thiès, Sénégal. Tel.: +221771541244, E-mail address sidym.dieng@univ-thies.sn

- Dr. Ziad Omran, Department of Pharmaceutical Chemistry, College of Pharmacy, Umm AlQura University, 21955 Makkah, Kingdom of Saudi Arabia. Tel.: +966 5 46461441; E-mail address: zhomran@uqu.edu.sa

- Pr. Thierry Vandamme, University of Strasbourg, CNRS 7199, Laboratoire de Conception et Application de Molécules Bioactives, équipe de Pharmacie Biogalénique, route du Rhin No.74, F-67401 Illkirch Cedex, France. Tel.: + 33 3 68 85 42 51, Fax: + 33 3 68 85 43 06; E-mail address: vandamme@unistra.fr

Short statistical summary:

Total number of words: 5313 (reference list excluded)

Total number of Figures: 5

Total number of Tables: 0

34 **ABSTRACT**

35 The purpose of this study was to develop Pickering water-in-oil nano-emulsions only
36 stabilized by Eudragit RL100 nanoparticles (NPs), in order to increase the nano-emulsion
37 stability and create a barrier to improve the drug encapsulation and better control the drug
38 release. The first part of this study was dedicated to investigating the nano-emulsion
39 formulation by ultrasonication and understanding the interfacial behavior and role of NPs in
40 the stabilization of the water/oil interface. The focus was on the surface coverage in the
41 function of the formulation parameters (volume fractions) to disclose the extents and
42 limitations of the process. The main physicochemical analysis of the Pickering nano-
43 emulsions was performed by dynamic light scattering and transmission electron microscopy.
44 On the other hand, the second experimental approach was dedicated to understanding the
45 interfacial behavior of the Eudragit RL100 NPs toward a model water/oil interface, using a
46 dynamic tensiometer with axisymmetric drop shape analysis. The study investigated the NPs'
47 adsorption, as well as their rheological behavior. The aim of this part was to reveal the main
48 phenomena that govern the interactions between NPs and the interface in order to understand
49 the origin of Pickering nano-emulsions' stability. The last part of the study was concerned
50 with the stability and *in vitro* release of a model encapsulated drug (ketoprofen) in a gastric
51 and simulated intestinal environment. The results showed that Pickering nano-emulsions
52 significantly improved the resistance to gastric pH, inducing a significantly slower drug
53 release compared to classical nano-emulsions' stabilized surfactants. These Pickering nano-
54 emulsions appear as a promising technology to modify the delivery of a therapeutic agent, in
55 the function of the pH, and can be, for instance, applied to the oral drug delivery of poorly
56 soluble drugs.

57

58 **Keywords:** Pickering, nano-emulsion, Eudragit RL100, nanoparticle, ketoprofen.

59

60 1- INTRODUCTION

61 Pickering's solid particle-stabilized emulsions were discovered by Ramsden and Pickering in
62 the 1900s and developed slowly until the 1980s [1,2]. Compared to surfactant-stabilized
63 emulsions, Pickering emulsions have shown the advantages of strong stabilization and very
64 good coalescence resistance due to the formation of a dense shell of solid particles
65 irreversibly adsorbed around water droplet emulsions. Pickering emulsions also have the
66 advantage of being nontoxic and environment-friendly and lower production costs [3–12].
67 Over the past decade, Pickering emulsions have generated considerable interest in research in
68 several areas—particularly in the cosmetic and pharmaceutical fields or food applications,
69 where surfactants often have undesirable effects (such as irritation and hemolytic behavior)
70 [13]. As a new drug delivery system, Pickering emulsions could facilitate dermal drug
71 delivery [14,15], increase the oral absorption of poorly water-soluble drugs [16,17] and to
72 improve the drug stability [18].

73 Recently, various Pickering nano-emulsions have been described [19–23]. They have average
74 droplet diameters in the range of 50 to 300 nm. [24,25] Such fine droplets mean that creaming
75 or gravity sedimentation becomes negligible, even over relatively long time scales. In
76 addition, the much larger surface area of the droplets leads to more active formulations
77 potentially advantageous for cosmetics [22], agri-food products [26,27], drug administration
78 [21] and food manufacturing applications [19,28,29].

79 The adsorption of solid particles at the water/oil interface is irreversible and strong. It leads to
80 the formation of a dense film and creates a barrier around the droplets, thus making the
81 nanodroplets extremely resistant to coalescence. The control of the properties of the
82 stabilizing particles due to the nature of the continuous phase can induce a change in the
83 wettability, and can therefore possibly provide a control of the droplet interface
84 destabilization and potentially a continuous release of drug. Energy related to the interactions
85 of the NPs with the interface, *i.e.* adsorption and desorption, is related to their respective
86 wetting by water and oil at interface [22]. Although the mechanisms involved in the stability
87 of Pickering emulsions are well described, the role the the nature of the particles and their
88 interfacial properties is still the subject of various opinions [30–33]. In some literature
89 reports, it has been shown that submicron particles, in some cases, only exhibit a limited
90 effect on the interfacial tension. Thus, they are rather considered a third phase located
91 between water and oil, with a negligible role on the interfacial energy [34]. To study the

92 stability of foams, Hunter *et al.* [34] studied in parallel the adsorption of hydrophobic silica
93 particles (~260 nm) and surfactants, onto an air/water interface. In that case, the NPs did not
94 impact on the value of the surface tension [34]. However, other authors have reported an
95 important effect of the particles on the interfacial tension. Kutuzov *et al.* [31], for instance,
96 showed that interfacial tension decreased with increased particle concentration, using
97 cadmium selenide (CdSe) particles at the toluene/water interface. In general, in the function
98 of the nature of the particles and the experimental conditions, nanoparticles (NPs) in
99 suspension can have a significant impact on surface tension or can be almost neutral [30–
100 33,35–37]. In the case of Pickering emulsions, several types of NPs were shown to be very
101 efficient stabilizers –such as CdSe NPs (1–8 nm) [38], silver NPs (1–5 nm) [39] or clay
102 particles (25–35 nm) [40]. The drop tensiometer is widely used to study the interfacial
103 tension and rheology of surfactant systems at liquid/liquid interfaces. It is interesting to note
104 that the debate on the interfacial effect and activity of NPs at liquid/liquid interfaces is still
105 ongoing, regarding whether they do not induce any modifications of the interfacial tension
106 and rheological properties after their adsorption [30–33,35–37] or their adsorption strongly
107 modifies the interfacial properties [41–44]. In fact, this debate might be likely due to the
108 infinite variabilities of the NPs' chemical and physicochemical properties.

109 The main goal of this study was to develop Pickering nano-emulsions stabilized by
110 Eudragit RL100 NPs as effective oral drug delivery systems. The choice of Eudragit RL 100
111 was done because it is widely used for *in vivo* formulations intended to the oral route, and it
112 is stable towards the physiological conditions encountered in the gastro-intestinal tract. To
113 achieve this aim, we used a polymeric stabilizer to formulate a new form of Pickering nano-
114 emulsions. As a model encapsulated drug, ketoprofen has been solubilized into the internal
115 phase of the nano-emulsions. This formula was intended to prolong the effect of ketoprofen
116 and thus reduce the frequency of administration. In addition, we studied the effect of NPs on
117 interfacial tension. In parallel, the study of the NPs' adsorption onto a model oil/water
118 interface was carried out on a drop tensiometer. This experimental approach provide the
119 kinetics of the NPs' adsorption and allow accessing the rheological properties of the NPs
120 monolayers. Interfacial rheology experiments were performed to characterize the phenomena
121 governing the particle adsorption at the interface and understand the strength of their surface
122 activity and their efficiency to stabilize the nano-emulsion droplets' interface. Further
123 characterizations were conducted to evaluate the nano-emulsion size and stability, along with

124 in vitro release studies of a model encapsulated drug (ketoprofen) performed in a simulated
125 gastric and intestinal medium (pH 1.2 and 6.8, respectively).

126

127

128 **2- EXPERIMENTAL SECTION**

129 **2-1 Materials**

130 Ketoprofen was purchased from Fagron S.A (Saint-Denis, France), and Eudragit[®] RL100
131 (Ammonio Methacrylate copolymer Type A NF) from Evonik Röhm GmbH Pharma
132 Polymers (Darmstadt, Germany). Acetone and cyclohexane analytical grades and Kolliphor[®]
133 ELP (nonionic PEGylated surfactant) were purchased from Sigma Aldrich. Medium chain
134 triglyceride compatible with the parenteral administration, Labrafac[®] WL1349 was obtained
135 from Gattefossé SA (Saint-priest, France), and pure water from a Millipore super-Q unit
136 (Millipore, Illkirch, France). All chemicals used were of analytical grades and used without
137 modification.

138

139 **2-2 Methods**

140 2-2-1 Preparation of NPs Eudragit RL100

141 Nanoparticles were prepared by nanoprecipitation method [45]. Eudragit RL100 was
142 dissolved in the internal phase containing acetone (50 mL) at room temperature (25°C). The
143 ratio of organic phase in the aqueous phase was (3:1). The resulting organic phase was
144 injected at the constant rate of 0.5 mL / min in aqueous phase (150 mL) containing 1% of
145 Kolliphor[®] ELP, under a gentl agitation at 300 rpm. Acetone was then removed using a
146 rotavapor.

147 The nanoparticle suspension is first concentrated by evaporating of a significant amount of
148 water (75 mL) and then washed for 48 hours. The NPs are then washed with MilliQ water by
149 dialysis Spectra-Por, regenerated cellulose, cutoff 8-12 kDa), in MilliQ water under gentle
150 stirring, and for 48 hours. Dialysate was changed once after 24h. Objective of this washing
151 stage is to remove the free surfactant (Kolliphor[®] ELP). These washed NPs suspensions were
152 used to prepare the nanoemulsions.

153

154 2-2-2 Preparation of Pickering nanoemulsions

155 The O/W nanoemulsions were formulated with 80 wt.% of aqueous phase containing the NPs
156 and 20 wt.% of Labrafac[®] WL1349 as oil phase. A premix is formulated using a mechanical
157 mixer (Ultraturrax, IKA T-25 digital) operating at 22400 rpm for 3min, at 25 °C. Then, the
158 nano-emulsion is generated by ultrasonication (Sonics Materials, Bio block 75043, Newtown,
159 MA, USA), 150 W, watt and 20 kHz, during 3 minutes (6 cycles of 10 s “on” and 20 s “off”).

160 2-2-3 NPs Eudragit and Pickering nanoemulsions characterizations

161

162 *2-2-3-1 Size distribution and ζ potential measurements*

163 Size distributions, polydispersity indexes (PDI) and zeta potentials were determined with a
164 NanoZS (Malvern Instruments, Orsay, France), by dynamic light scattering (DLS), and
165 measurement of the electrophoretic mobility of the nano-emulsion droplets, respectively. All
166 experiments were performed in triplicate.

167

168 *2-2-3-2 Transmission electron microscopy*

169 Transmission electron microscopy (TEM) characterization were performed using Philips
170 Morgagni 268D microscope operating at 70 kV. No staining agent were used and the samples
171 were diluted 100 times with MilliQ water. A drop of the sample, beforehand deposited on a
172 support (carbon type-A, 300 mesh, copper, Inc. Redding, PA), was dried at 40°C.

173

174 *2-2-3-3 Axisymmetric Drop Shape Analysis (ADSA)*

175 Interfacial properties were assessed by axisymmetric drop shape analysis using a dynamic
176 drop tensiometer (Teclis, Longessaigne, France). The first experiment was the study of a
177 rising drop (drop of cyclohexane in water) (8 microliters) maintained at constant volume and
178 temperature. Aqueous phase was either the NPs 40 nm suspension) and MilliQ as control.
179 The second type of experiment was the pendant drop configuration (drop of aqueous NPs
180 suspension in cyclohexane. The interfacial tension was determined from the drop profile and
181 analyzed using a CCD camera integrated to the setup. The drop profile results from a

182 competition between gravity and capillary forces tend to elongate the drop profile whereas
183 the capillary forces (which depend on the interfacial tension) tend to round the drop profile.
184 As a result, its Laplacian shape gave the values of interfacial area and surface tension. All
185 experiments were performed at 25 °C, in triplicate.

186

187 *2-2-3-4 Interfacial rheology*

188 The dilatational elastic modulus was assessed by the relationship between surface tension and
189 interfacial area (imposed though a sinusoidal profile). The experiment begins when the
190 surface tension is stabilized, and reproduced over a large frequency range (0.0033 Hz, 0.005
191 Hz, 0.0066 Hz, 0.01 Hz, 0.016 Hz, 0.022 Hz, 0.033 Hz, 0.05 Hz, 0.066 Hz, and 0.1 Hz).
192 Experiments were conducted in order to get Bond number around 0.2-0.25, and sinusoid
193 amplitudes around 10% of the drop volume [46–48] . Temperatures was maintained at 20°C,
194 and experiments were performed three times.

195

196 *2-2-4 In vitro release study*

197 As a model drug soluble in oil, ketoprofen was encapsulated in Pickering nanoemulsions at
198 0.33 mg/mL. The solubilization of ketoprofen in Labrafac[®] WL 1349 was carried out by
199 using a thermomixer (Thermomixer C Eppendorf) at 37°C for 15 min. The ketoprofen release
200 profiles were characterized by dialysis (2 mL of loaded nanoemulsions at a concentration in
201 solution equal to 0.33 mg/mL, and the dialysis tubing as Spectra-Por, regenerated cellulose,
202 cut-off: 12-14 kDa). Dialysis was done in 300 mL, magnetically stirred at 100 rpm. The first
203 time period was fixed at 30 min in simulated gastric fluid at pH = 1.2 as a release medium.
204 Then, 9 hours in PBS at pH = 6.8 [49,50]. Aliquots of 5 mL were regularly collected from the
205 dissolution medium, and analyzed by UV spectrophotometry (UV 2400 PC series
206 SHIMADZU spectrophotometer, Kyoto, Japan). Absorbance values were monitored in a
207 quartz cuvette at 258.5 nm and 260 nm for simulated gastric fluid and PBS respectively. Sink
208 conditions were maintained by replacing 5 mL of the release medium with fresh media at
209 each sampling point. This allowed the determination of the cumulative drug amounts released
210 from nanoemulsions. UV-vis absorption spectra of the Pickering nanoemulsions were
211 recorded on sample solutions using a UV 2400 PC series SHIMADZU spectrophotometer

212 with a wavelength range of 180 – 500 nm at 0.2 nm sampling interval. All experiments were
213 performed in triplicate.

214

215 **3- RESULTS AND DISCUSSIONS**

216 **3-1 Characterizations of NPs and Pickering nano-emulsions**

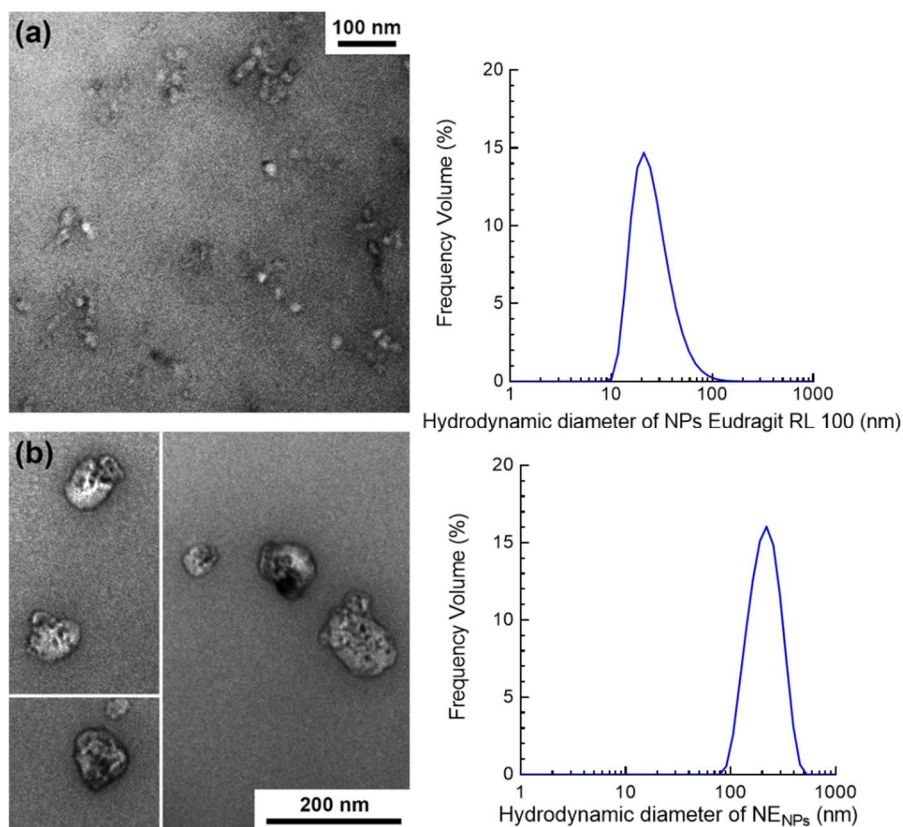
217 The size of the NPs depends on the composition of the aqueous and organic phases used
218 during the preparation. Eudragit RL100 NPs were prepared and they showed a size
219 distribution having a log-normal profile, centered on a diameter of 40 nm (see Fig. 1). The
220 value of the polydispersity index (PDI) was equal to 0.098, which implied a good
221 monodispersity of the suspension. Finally, the measured zeta potential was equal to +35 mV.

222 NPs of sizes 40 nm were formulated. The suspension of the NPs was used to prepare the
223 Pickering nano-emulsions. A ratio (4:1) (suspension of NPs in Labrafac® WL1349) was used.
224 The appearance of the formulation was transparent white. The manufacturing protocol was
225 highly reproducible. The size of the Pickering NPs was an average of 220 nm. A good
226 polydispersity index (0.184) was observed for the preparation (4:1). The zeta potential
227 obtained was of the order of +35 mV and was the same as for the polymeric NPs prepared.
228 Morphological characterizations of the NPs and nano-emulsions were performed by
229 Transmission electron microscopy (TEM) (see Fig. 1). NPs (Fig. 1 (a)) appeared as round
230 spheres with a size coherent with the dynamic light scattering (DLS) results and a distribution
231 centered on a diameter of 40 nm. Some were isolated in the carbon support while others were
232 aggregated as clusters. This usually happens during sample drying. As they were
233 nanoprecipitated, the polymer NPs were in a glassy state and showed a hypo-contrast, which
234 is generally the opposite of what happens in lipid particles [51]. On the other hand, nano-
235 emulsions (Fig. 1 (b)) showed larger particles that were still in line with the DLS results
236 (150–200 nm), and a hypo-contrast that is likely related to the presence of polymer particles
237 at the droplet's interface.

238 These observations appear to be in coherence with the literature reports that have presented
239 Pickering emulsions stabilized by solid particles [33,52]. Thus, it seems to corroborate the
240 fact that the nano-emulsions formulated were effectively stabilized with Eudragit RL100
241 NPs. Nano-emulsion droplets appeared well differentiated from each other, globally
242 conserving their shape even after vacuum establishment during the TEM observations (*i.e.*

243 not spread onto the carbon support as reported with simple nano-emulsions [51]). This means
244 that the interface was stabilized by aggregated NPs, creating a rigid film that acted as a
245 physical barrier against flocculation and coalescence.

246



247

248 **Figure 1:** Physico-chemical characterization of the polymer nanoparticles (a) and Pickering nano-emulsions (b),
249 by transmission electron microscopy (left row) and dynamic light scattering (right row).

250 These observations appears in coherence with the literature reports that presented Pickering
251 emulsions stabilized by solid particles [33,52], thus seems to corroborate the fact that the
252 nano-emulsions formulated are effectively stabilized with Eudragit RL100 NPs. Nano-
253 emulsion droplets appear well differentiated each other, globally conserving their shape even
254 after vacuum establishment during the TEM observations (*i.e.* not spread onto the carbon
255 support as reported with simple nano-emulsions [51]). This means that the interface is
256 stabilized by aggregated NPs, creating a rigid film that acts as a physical barrier against
257 flocculation and coalescence.

258 **3-2 Interfacial coverage**

259 The coating of a spherical droplet with smaller NPs generally results in thick and compact
260 shells [44,53–55]. To study and confirm this hypothesis, the surface coverage was followed

261 in the function of the volume fraction of the dispersed phase. The NP packing around a larger
262 particle can be, in the function of the particle properties, either a compact monolayer [56] or a
263 thick multilayer particle shell [57]. In this section, we propose studying the emulsion surface
264 coverage by NPs, through a methodology that involves investigating the relationship between
265 the size of the nano-emulsions formulated in the function of the volume fraction of dispersed
266 phase (*i.e.* of oil) and estimating the emulsion coverage as the maximum number of NPs
267 entrapped at the droplet interface. At constant NPs size and concentration in the aqueous
268 phase, different Pickering nano-emulsions formulations were prepared by increasing the
269 value of the volume fraction of the dispersed phase. The values of the nano-emulsion
270 hydrodynamic diameter (as reported in Fig. 2 (a)) revealed the gradual increase of the nano-
271 emulsion size –an expected result since the number of NPs is constant in the bulk. Then, the
272 corresponding total number of nano-emulsion droplets N_{NE-tot} in the suspension (see
273 Fig. 2 [b]) decreased initially but finally stabilizes as the oil volume further increased. As the
274 additional dispersed phase was added, the total specific surface of the oil nano-emulsion size
275 decreased and the number of particles fell. The stabilization means an equilibrium was
276 reached and might be the sign of the total consumption of the NPs for the interface
277 stabilization. This result is coherent with a lack of stabilizing agents, all NPs being already
278 trapped at interface.

279 Therefore, assuming that at equilibrium, all the available oil/water interface is occupied by
280 the NPs and trapped at the interface at their largest effective cross-section (S_{NPs}), the number
281 of NPs that can possibly adsorb on the nano-emulsion droplet interface, $N_{NPs/NE-I}$, is evaluated
282 as the ratio between the area of a single nano-emulsion droplet A_{NE-I} and the section of a solid
283 lipid NP S_{NPs} (see Fig. 2 (c)). Thus, $N_{NPs/NE-I}$ increase with the volume fraction of the
284 dispersed phase (an expected behavior as the droplet size increases) (Fig. 6 (a)). Finally, the
285 total number of NPs adsorbed onto the nano-emulsions droplets, $N_{NPs/NE-tot}$, as reported in
286 Fig. 2 (d), showed a constant increase with the further addition of oil. This means that
287 maximum interfacial coverage was not reached even at the highest volume fraction.

288 The average droplet diameter is proportional to their coverage rate, and inversely
289 proportional to the total number of stabilizing particles. A similar relationship between the
290 final diameter D_f and the mass of particles has been proposed in literature [4], based on the
291 assumption that the particles form a monolayer in a compact hexagonal stack at the water-oil
292 interface.

293 The “limited coalescence” is a phenomenon that occurs when the interfacial area of all the
294 droplets is much greater than the surface the stabilizing particles could cover. Accordingly, as
295 the adsorption is irreversible, coalescence reduces the interface up to it is equal to the surface
296 that the adsorbed particles can cover. Thus, if the volume fraction of dispersed phase is
297 increased, the limited coalescence will govern the final stabilization droplet size.

298

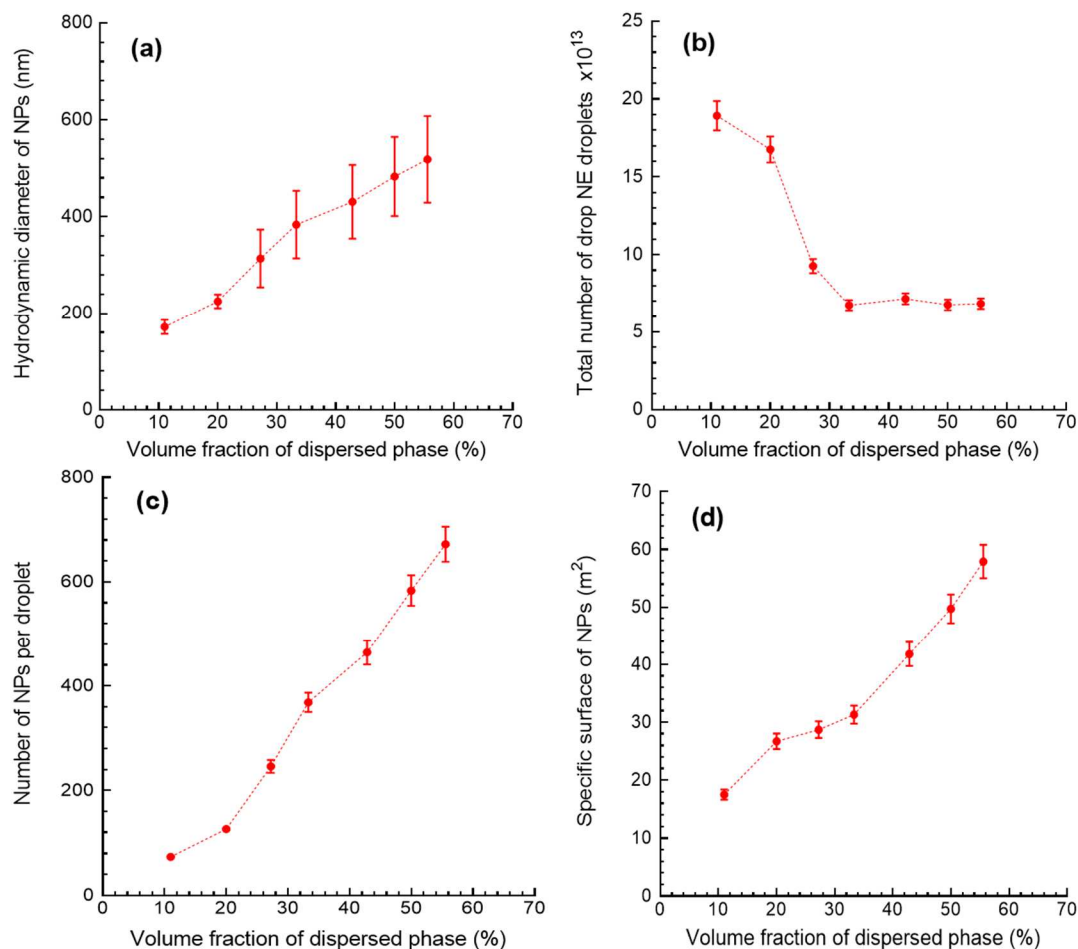
299 It follows, therefore, that the nano-emulsions formed were effectively stabilized by NPs,
300 which is coherent with the idea that these Pickering nano-emulsions are stabilized by a dense
301 NPs layer. This was confirmed by the TEM observations (Fig. 1 (a)), which showed an
302 important concentration of Eudragit RL 100 NPs colocalized with the nano-emulsion
303 droplets. Eventually, one can imagine such a layer constituting a barrier against the release of
304 encapsulated active ingredients. These dialyzed NPs were characterized by tensiometry and
305 interfacial rheology.

306

307

308

309



310

311 **Figure 2:** Study of the NPs coverage of the nano-emulsion droplets, in function of the volume fraction of
 312 dispersed phase (continuous phase is water aqueous phase containing NPs, and the dispersed phase is oil
 313 composed of MCT). (a) Hydrodynamic diameter of the nano-emulsions, (b) number of the nano-emulsion
 314 droplets, (c) number of NPs adsorbed at the interface of a single nano-emulsion droplet, and (d) number of NPs
 315 adsorbed onto all the nano-emulsions droplets, $n=3$.

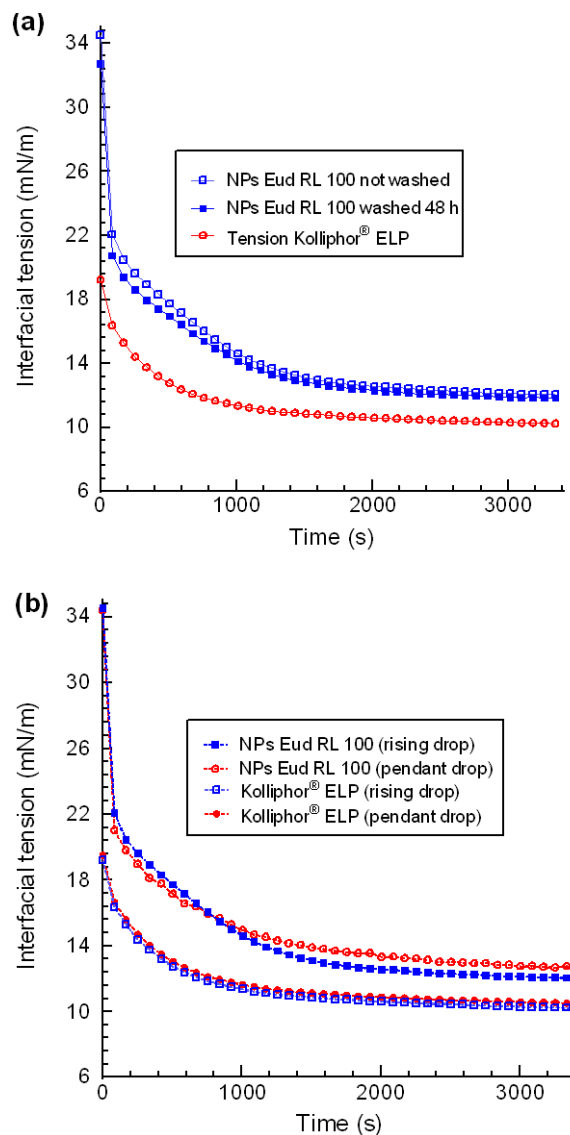
316

317 **3-3 Interfacial tension**

318 To better understand the stabilization mechanism of nano-emulsions, the adsorption kinetics
 319 of polymeric NPs onto a model interface was studied. To this end, a model interface
 320 $C_6H_{12}/water$ (aqueous NPs suspension) was created and the interfacial tension was followed-
 321 up. The first control experiment was conducted to show that the interfacial effect is
 322 effectively due to the NPs adsorbed at the interface and not the residual unwashed
 323 surfactants. In this experiment (see Fig. 3 (a)), a concentration of $5 \mu L/mL$ (*i.e.* $5 \mu L$ of a
 324 solution of NPs diluted in 1 mL of MilliQ water) of washed (*i.e.* before dialysis) and
 325 unwashed (*i.e.* after 48 hrs of dialysis) NPs and surfactant (at $3 \cdot 10^{-3} mg/mL$ – a concentration
 326 corresponding to the one used in the NPs formulation) were compared (rising drop

327 configuration). The results showed that surfactant alone has a more important effect on the
328 surface tension than the two other suspensions of NPs stabilized around 2000 s at 11 mN/m.
329 On the other hand, washed and unwashed NPs suspension exhibited a very similar profile,
330 also stabilized around 2000 s but slightly higher than the pure surfactant at about 2 mN/m. In
331 fact, in the case of unwashed samples, both NPs and the free surfactants are liable to be active
332 at interface. However, as the surface tension profile almost superimposed to the one of
333 washed NPs, we can conclude that interfacial behavior is dominated by the NPS, *i.e.* the
334 interfacial composition is predominantly composed of NPs. The second control experiment
335 (see Fig. 3 (b)) compared the NPs to the free surfactant (at the concentration initially used for
336 their formulation) in the cyclohexane rising and water pendant drop configurations. As
337 expected, the values were close, irrespective of the configuration, and similar to those
338 observed in Figure 3 (a). However, when the curves profiles were exactly superimposed for
339 the surfactants, they appeared very slightly different regarding the NPs.

340



341

342 **Figure 3:** Study of the NPs adsorption of NPs on model C_6H_{12} / MilliQ water interface (aqueous suspension of
 343 NPs) at 25°C. (a) Comparison of washed and not washed NPs (40 nm), and free surfactants (Kolliphor[®] ELP at
 344 $3 \cdot 10^{-3}$ mg/mL), for the rising drop configuration. (b) Comparison of NPs (40 nm) washed, and free surfactants
 345 (Kolliphor[®] ELP at $3 \cdot 10^{-3}$ mg/mL), for pendant and rising drop configurations.

346

347 **3-4 Interfacial dilatational viscoelasticity measurement**

348 Dilatational viscoelasticity was performed according to the similar experimental
 349 configuration used for the surface tension measurements at the water/cyclohexane interface
 350 and the concentrations mentioned in the previous section with washed NPs. Pendant and
 351 rising drops were also compared. This experiment, through the evaluation of the complex
 352 dilatational elasticity E^* (with $E^* = E' + iE''$), will provide the values of the conservative
 353 (E') and dissipative (E''), globally referring to the intermolecular interactions at the interface
 354 and the interactions of the molecules at the interface with the subphases, respectively. These

355 data were obtained by imposing a sinusoidal variation of the volume on the drop and
356 measuring the response of the drop as regards the surface tension (beginning after the
357 stabilization shown in Fig. 3) for the rising drop.

358 To analyze these results and understand the limiting phenomena, the classical Lucassen and
359 van den Tempel (LvdT) model was applied. LvdT is widely described in the literature [52–
360 54] and accounts for a system in which the diffusion is the limiting process governing the
361 interactions with the interface, that is, interfacial adsorption and desorption are slower and/or
362 stronger than interactions at the interface between adsorbed compounds. LvdT is validated
363 when both conservative and dissipative contributions satisfy the following equations:

$$364 \quad E' = E_0 \frac{1+\Omega}{1+\Omega+\Omega^2} \quad (\text{Eq. 1})$$

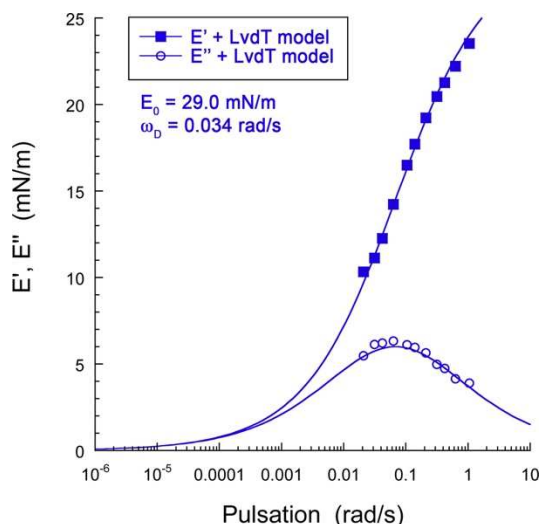
$$365 \quad E'' = E_0 \frac{\Omega}{1+\Omega+\Omega^2} \quad (\text{Eq. 2})$$

366 where E_0 is the limit elastic modulus at very high frequency (for which the area increases
367 only “dilutes” the NPs at the interface), Ω is the reduced angular frequency given by $\Omega =$
368 $\left(\frac{\omega_D}{\omega}\right)^{1/2}$, and ω_D being the characteristic angular diffusion frequency representing the frontier
369 between viscous friction regimes for $\omega < \omega_D$ and elastic regime for $\omega > \omega_D$. The results are
370 reported in Figure 4, showing the raw values of E' and E'' along with the LvdT extrapolation.
371 For comparison, similar experiments done in the pendant drop configurations were shown in
372 the Supplementary Information section (Fig. S2).

373

374

375



376

377 **Figure 4:** Interfacial rheology study on the model water (containing NPs) / C₆H₆ interface, rising drop
 378 configuration. Experimental values of conservative (E') and dissipative (E'') modulus are extrapolated
 379 according to the Lucassen and van den Tempel model described by Eq. 1 and Eq. 2, respectively. and the limit
 380 elastic modulus E_0 and the characteristic angular diffusion frequency ω_D are reported in the figures ($n = 3$).

381

382 These results show a high impact of the pulsation on the values of the conservative
 383 contribution E' . In comparison, E'' shows more regular values around 5 mN/m. These
 384 experimental data can be successfully modeled with the LvdT model, ($R^2 = 0.995$ and
 385 0.926 , for E' and E'' , respectively), giving a limit elasticity value $E_0 = 29.0$ mN/m and a
 386 characteristic angular diffusion frequency $\omega_D = 0.034$ rad/s. This concordance confirms that
 387 the NPs are relatively mobile, able to migrate from the interface to the bulk surrounding
 388 subphases, and the diffusion is effectively the limiting phenomenon. In fact, during the
 389 surface expansion of the droplet, adsorption of additional NPs is allowed on the free
 390 interfacial regions; and as the droplet contract, the NPs are gradually expelled. In the present
 391 case, only adsorption/desorption phenomena dominated. We can also consider that NPs do
 392 not form aggregate or cluster each other when they are confined at the interface (or if any,
 393 only with loose interactions).

394 The bridge with the stability of Pickering nano-emulsion come with the confirmation of the
 395 marked adsorption of the NPs at the droplet interface (during the sonication and the droplet
 396 formation), first revealed by an impact on the surface tension, and then by the fact that the
 397 NPs mobility toward interface is the main phenomena driving their interfacial behavior. On
 398 the other hand, increasing the frequency strongly increases the conservative elasticity,
 399 tending to $E_0 = 29.0$ mN/m. In those conditions, the NPs are retained at the interface because
 400 their diffusion is not fast enough to counterbalance the adsorption energy. However, after the

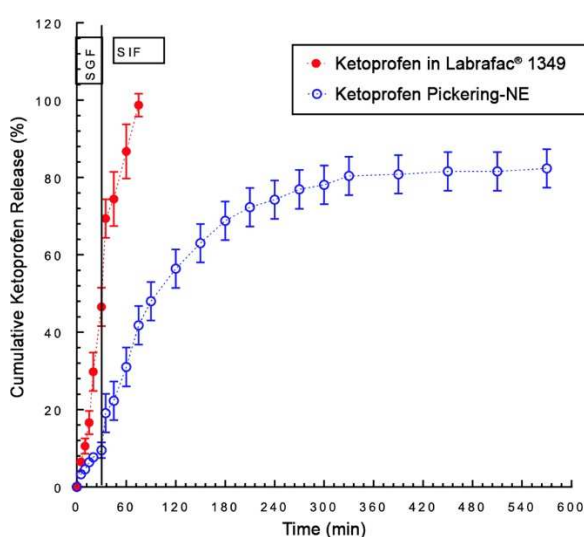
401 formulation of nano-emulsions (i.e., once the droplets are formed and ultrasonication
402 stopped), we can consider the system below the elastic regime ($\omega < \omega_D = 0.034$ rad/s),
403 without further change in the droplet area, and the adsorption energy stably anchoring the
404 NPs at the interface.

405 Interestingly, when the rheological behavior is compared to the pendant drop configuration
406 (Fig. S2 in the *Supplementary information* section), the interfacial behavior is partly similar
407 and the LvdT model can be also applied with some differences. The first one lies in the LvdT
408 parameters values, very close for E_0 , arising equal to 27.3 mN/m for pendant drop (and was
409 29.0 mN/m for rising drop), but divided-up for ω_D , equal to 0.016 rad/s for pendant drop (and
410 was 0.034 rad/s for rising drop). On the other hand, for the lower frequencies
411 ($\omega < 0.042$ rad/s), the values of E' and E'' literally shows a jump (indicated by arrows in
412 Fig. S2) that makes these conditions out of the LvdT model, and that is important since it
413 means that the diffusion is not anymore the NPs limiting process driving the interfacial
414 phenomena but that NPs now strongly interact each other. When at the molecular level the
415 interfacial curvature cannot have any influence on the interfacial phenomena, when
416 increasing the scale with NPs sizing above 200 nm, it appears important. In addition, as the
417 polymeric NPS herein studied stabilized oi-in-water nano-droplets, their location at the
418 water/oil interface is are likely shifted towards water, meaning that the rising configuration
419 (oil-in-water) is favorable and the pendant configuration (water-in-oil) is unfavorable.
420 Unfavorable, revealed in Fig. S2, means that their confinement is increased, results in the
421 creation of strong interparticle interactions when the interfacial deformation is slowest (*i.e.*
422 when LvdT model is not verified). This interesting detail disclose the fact that NPs able
423 nevertheless able to create a strong network, but when stabilizing the nano-emulsions is
424 seems not effective, along with being an efficient stabilizing agent for nano-emulsions.

425 **3-5 In vitro release studies**

426 The choice of Eudragit[®] RL 100 in the fabrication of the stabilizing NPs was made because
427 of their ability to form a strong barrier against the release of ketoprofen over time and the
428 sensitivity of the polymer to the pH—the potential to induce a controlled release as a function
429 of the location in the gastrointestinal tract. Ketoprofen an acidic drug with a pKa of 4.45,
430 ketoprofen has poor aqueous solubility in acidic media (0.13 mg/ml at pH 1.2) [61,62], and
431 considerably higher solubility at neutral environment (40.76 mg/ml at pH 6.8) [63]. As
432 reported in Figure 5, the ketoprofen release is overall rapid—100% of the drug was released

433 within 2 h. By comparing the Pickering nano-emulsions and the control (ketoprofen in
434 Labrafac[®] WL 1349 at the same concentration), it clearly appeared that the stabilization by
435 Eudragit RL100 NPs significantly prolonged the ketoprofen release. In fact, for the control
436 emulsion, 100% of the drug was leaked after only 1 h, while for Pickering nano-emulsions
437 about 30% was leaked, and only 10% released during the 30 min at pH 1.2, with a gradual
438 increase in the release rate at pH 6.8. Approximately, 70% of the drug has leaked after 5 h at
439 pH 6.8, finally reaching 82% after 6 h. A cutting-edge effect on the drug release profile was
440 obtained due to the stabilization of the nano-emulsion droplets by pH-sensitive NPs, which is
441 in line with the objective of this study, opening the way for designing innovations in
442 controlled drug release dosage forms [55,64,65].



443
444 **Figure 5:** The release of ketoprofen encapsulated in the Labrafac[®] WL 1349 (red curve), and compared with
445 Pickering nano-emulsions (blue curve: 80 wt.% of aqueous phase containing the NPs and 20 wt.% of Labrafac[®]
446 WL1349; concentration of ketoprofen in the solution equal to 0.33 mg/mL). The first part presents a release in
447 SGF (pH 1.2) followed by SIF (pH 6.8) as indicated in the figure.

448 449 **4- CONCLUSION**

450 This study suggests a new formulation of nano-emulsions stabilized solely by Eudragit
451 RL100 NPs. Solutions for formulating Pickering nano-emulsions have been found—that is,
452 lipid droplets only stabilized with polymeric NPs (Eudragit[®] RL100). Pickering nano-
453 emulsions are safe and very stable, but they are generally fabricated at a microscale. The
454 formulation itself uses neither surfactants nor amphiphilic polymers, only NPs as stabilizers.
455 This is the first innovation of this study. NPs generated by nanoprecipitation sized around
456 40 nm and the nano-emulsions formulations around 220 nm showing high stability. The first
457 part of this study focused on the characterization of these nano-emulsions to prove that they

458 are effective Pickering nano-emulsions and characterize the extents and limits of the nano-
459 emulsion formulation process and the surface coverage in the function of the volume fraction
460 of oil. The second part of the study focused on the interfacial behavior of the NPs at a model
461 water/oil interface, analyzed through the axisymmetric drop shape analysis. The influence of
462 the NPs on the surface tension and dilatational rheology was measured and the rheological
463 behavior efficiently analyzed with the classical LvdT model. The results showed that the NPs
464 were efficiently trapped at the oil/water interface; even for the control experiment in the
465 presence of surfactants, the NPs had a predominant effect once trapped. The surface coverage
466 revealed a compact layer surrounding the lipid droplets; this was confirmed by TEM. The
467 application of the LvdT model to the rheology results also confirmed that NPs were
468 efficiently adsorbed and that the adsorption/desorption predominated over interparticle
469 interactions. This signifies that the NPs formed did not create an aggregated shell but were
470 strongly anchored at the interface. Finally, we have shown that the release of a model
471 lipophilic drug (ketoprofen) was significantly slowed down when nano-emulsions are
472 stabilized with NPs, in comparison with surfactants used as the control. These last results
473 fulfilled the objectives and specifications of the study, but the comprehensive
474 physicochemical characterization carried out in this study opened new perspectives on the
475 formulation of Pickering nano-emulsions.

476

477 **Acknowledgments**

478 The authors would like to acknowledge the financial support provided by King Abdulaziz
479 City for Science and Technology (KACST), Grant no. 14-MED1472-10.

480

481

482

483 **References**

- 484 [1] S.U. Pickering, CXCVI.—Emulsions, *J. Chem. Soc., Trans.* 91 (1907) 2001–2021.
485 <https://doi.org/10.1039/CT9079102001>.
- 486 [2] w Ramsden, Separation of solids in the surface-layers of solutions and ‘suspensions’
487 (observations on surface-membranes, bubbles, emulsions, and mechanical
488 coagulation).—Preliminary account, *Proceedings of the Royal Society of London.* 72
489 (1904) 156–164. <https://doi.org/10.1098/rspl.1903.0034>.
- 490 [3] S. Abend, N. Bonnke, U. Gutschner, G. Lagaly, Stabilization of emulsions by
491 heterocoagulation of clay minerals and layered double hydroxides, *Colloid & Polymer*
492 *Science.* 276 (1998) 730–737. <https://doi.org/10.1007/s003960050303>.

- 493 [4] S. Arditty, C.P. Whitby, B.P. Binks, V. Schmitt, F. Leal-Calderon, Some general
494 features of limited coalescence in solid-stabilized emulsions, *The European Physical*
495 *Journal E*. 11 (2003) 273–281. <https://doi.org/10.1140/epje/i2003-10018-6>.
- 496 [5] B.P. Binks, S.O. Lumsdon, Pickering Emulsions Stabilized by Monodisperse Latex
497 Particles: Effects of Particle Size, *Langmuir*. 17 (2001) 4540–4547.
498 <https://doi.org/10.1021/la0103822>.
- 499 [6] B.P. Binks, S.O. Lumsdon, Stability of oil-in-water emulsions stabilised by silica
500 particles, *Physical Chemistry Chemical Physics*. 1 (1999) 3007–3016.
501 <https://doi.org/10.1039/a902209k>.
- 502 [7] S.A.F. Bon, P.J. Colver, Pickering Miniemulsion Polymerization Using Laponite Clay
503 as a Stabilizer, *Langmuir*. 23 (2007) 8316–8322. <https://doi.org/10.1021/la701150q>.
- 504 [8] C.A.L. Colard, R.F.A. Teixeira, S.A.F. Bon, Unraveling Mechanistic Events in Solids-
505 Stabilized Emulsion Polymerization by Monitoring the Concentration of Nanoparticles
506 in the Water Phase, *Langmuir*. 26 (2010) 7915–7921. <https://doi.org/10.1021/la904817f>.
- 507 [9] Z.-G. Cui, K.-Z. Shi, Y.-Z. Cui, B.P. Binks, Double phase inversion of emulsions
508 stabilized by a mixture of CaCO₃ nanoparticles and sodium dodecyl sulphate, *Colloids*
509 *and Surfaces A: Physicochemical and Engineering Aspects*. 329 (2008) 67–74.
510 <https://doi.org/10.1016/j.colsurfa.2008.06.049>.
- 511 [10] T.S. Horozov, B.P. Binks, Particle-Stabilized Emulsions: A Bilayer or a Bridging
512 Monolayer?, *Angewandte Chemie International Edition*. 45 (2006) 773–776.
513 <https://doi.org/10.1002/anie.200503131>.
- 514 [11] D.E. Tambe, M.M. Sharma, Factors Controlling the Stability of Colloid-Stabilized
515 Emulsions, *Journal of Colloid and Interface Science*. 157 (1993) 244–253.
516 <https://doi.org/10.1006/jcis.1993.1182>.
- 517 [12] A. Tsugita, S. Takemoto, K. Mori, T. Yoneya, Y. Otani, Studies on emulsions stabilized
518 with insoluble montmorillonite-organic complexes, *Journal of Colloid and Interface*
519 *Science*. 95 (1983) 551–560. [https://doi.org/10.1016/0021-9797\(83\)90214-X](https://doi.org/10.1016/0021-9797(83)90214-X).
- 520 [13] M. Rayner, D. Marku, M. Eriksson, M. Sjöö, P. Dejmek, M. Wahlgren, Biomass-based
521 particles for the formulation of Pickering type emulsions in food and topical
522 applications, *Colloids and Surfaces A: Physicochemical and Engineering Aspects*. 458
523 (2014) 48–62. <http://dx.doi.org/10.1016/j.colsurfa.2014.03.053>.
- 524 [14] F. Laredj-Bouezg, M.-A. Bolzinger, J. Pelletier, Y. Chevalier, Pickering emulsions
525 stabilized by biodegradable block copolymer micelles for controlled topical drug
526 delivery, *Int J Pharm*. 531 (2017) 134–142.
527 <https://doi.org/10.1016/j.ijpharm.2017.08.065>.
- 528 [15] M. Wahlgren, J. Engblom, M. Sjöö, M. Rayner, The use of micro- and nanoparticles in
529 the stabilisation of pickering-type emulsions for topical delivery, *Curr Pharm*
530 *Biotechnol*. 14 (2013) 1222–1234.
- 531 [16] S. Simovic, H. Hui, Y. Song, A.K. Davey, T. Rades, C.A. Prestidge, An oral delivery
532 system for indomethacin engineered from cationic lipid emulsions and silica
533 nanoparticles, *J Control Release*. 143 (2010) 367–373.
534 <https://doi.org/10.1016/j.jconrel.2010.01.008>.
- 535 [17] A. Tan, S. Simovic, A.K. Davey, T. Rades, C.A. Prestidge, Silica-lipid hybrid (SLH)
536 microcapsules: a novel oral delivery system for poorly soluble drugs, *J Control Release*.
537 134 (2009) 62–70. <https://doi.org/10.1016/j.jconrel.2008.10.014>.
- 538 [18] N.G. Eskandar, S. Simovic, C.A. Prestidge, Chemical stability and phase distribution of
539 all-trans-retinol in nanoparticle-coated emulsions, *Int J Pharm*. 376 (2009) 186–194.
540 <https://doi.org/10.1016/j.ijpharm.2009.04.036>.

- 541 [19] D.J. McClements, J. Rao, Food-grade nanoemulsions: formulation, fabrication,
542 properties, performance, biological fate, and potential toxicity, *Crit Rev Food Sci Nutr.*
543 51 (2011) 285–330. <https://doi.org/10.1080/10408398.2011.559558>.
- 544 [20] K.H. Persson, I.A. Blute, I.C. Mira, J. Gustafsson, Creation of well-defined particle
545 stabilized oil-in-water nanoemulsions, *Colloids and Surfaces A: Physicochemical and*
546 *Engineering Aspects.* 459 (2014) 48–57. <https://doi.org/10.1016/j.colsurfa.2014.06.034>.
- 547 [21] N.Y. Rapoport, A.M. Kennedy, J.E. Shea, C.L. Scaife, K.-H. Nam, Controlled and
548 targeted tumor chemotherapy by ultrasound-activated nanoemulsions/microbubbles, *J*
549 *Control Release.* 138 (2009) 268–276. <https://doi.org/10.1016/j.jconrel.2009.05.026>.
- 550 [22] O. Sonnevile-Aubrun, J.-T. Simonnet, F. L’Alloret, Nanoemulsions: a new vehicle for
551 skincare products, *Adv Colloid Interface Sci.* 108–109 (2004) 145–149.
552 <https://doi.org/10.1016/j.cis.2003.10.026>.
- 553 [23] T. Tadros, P. Izquierdo, J. Esquena, C. Solans, Formation and stability of nano-
554 emulsions, *Adv Colloid Interface Sci.* 108–109 (2004) 303–318.
555 <https://doi.org/10.1016/j.cis.2003.10.023>.
- 556 [24] Z. Du, Q. Li, J. Li, E. Su, X. Liu, Z. Wan, X. Yang, Self-assembled egg yolk peptide
557 micellar nanoparticles as a versatile emulsifier for food-grade oil-in-water pickering
558 nanoemulsions, *Journal of Agricultural and Food Chemistry.* 67 (2019) 11728–11740.
559 <https://doi.org/10.1021/acs.jafc.9b04595>.
- 560 [25] D.J. Kang, H. Bararnia, S. Anand, Synthesizing Pickering Nanoemulsions by Vapor
561 Condensation, *ACS Appl Mater Interfaces.* 10 (2018) 21746–21754.
562 <https://doi.org/10.1021/acsami.8b06467>.
- 563 [26] Z. Du, C. Wang, X. Tai, G. Wang, X. Liu, Optimization and Characterization of
564 Biocompatible Oil-in-Water Nanoemulsion for Pesticide Delivery, *ACS Sustainable*
565 *Chem. Eng.* 4 (2016) 983–991. <https://doi.org/10.1021/acssuschemeng.5b01058>.
- 566 [27] J. Santos, L.A. Trujillo-Cayado, N. Calero, M.C. Alfaro, J. Muñoz, Development of
567 eco-friendly emulsions produced by microfluidization technique, *Journal of Industrial*
568 *and Engineering Chemistry.* 36 (2016) 90–95.
569 <https://doi.org/10.1016/j.jiec.2016.01.024>.
- 570 [28] A. Gupta, H.B. Eral, T.A. Hatton, P.S. Doyle, Nanoemulsions: formation, properties and
571 applications, *Soft Matter.* 12 (2016) 2826–2841. <https://doi.org/10.1039/c5sm02958a>.
- 572 [29] C. Solans, P. Izquierdo, J. Nolla, N. Azemar, M. Garcíacelma, Nano-emulsions, *Current*
573 *Opinion in Colloid & Interface Science.* 10 (2005) 102–110.
574 <https://doi.org/10.1016/j.cocis.2005.06.004>.
- 575 [30] A. Drelich, F. Gomez, D. Clause, I. Pezron, Evolution of water-in-oil emulsions
576 stabilized with solid particles, *Colloids and Surfaces A: Physicochemical and*
577 *Engineering Aspects.* 365 (2010) 171–177.
578 <https://doi.org/10.1016/j.colsurfa.2010.01.042>.
- 579 [31] S. Kutuzov, J. He, R. Tangirala, T. Emrick, T.P. Russell, A. Böker, On the kinetics of
580 nanoparticle self-assembly at liquid/liquid interfaces, *Phys. Chem. Chem. Phys.* 9
581 (2007) 6351–6358. <https://doi.org/10.1039/B710060B>.
- 582 [32] S. Levine, B.D. Bowen, S.J. Partridge, Stabilization of emulsions by fine particles II.
583 capillary and van der Waals forces between particles, *Colloids and Surfaces.* 38 (1989)
584 345–364. [https://doi.org/10.1016/0166-6622\(89\)80272-0](https://doi.org/10.1016/0166-6622(89)80272-0).
- 585 [33] E. Vignati, R. Piazza, T.P. Lockhart, Pickering Emulsions: Interfacial Tension,
586 Colloidal Layer Morphology, and Trapped-Particle Motion, *Langmuir.* 19 (2003) 6650–
587 6656. <https://doi.org/10.1021/la034264l>.
- 588 [34] T.N. Hunter, R.J. Pugh, G.V. Franks, G.J. Jameson, The role of particles in stabilising
589 foams and emulsions, *Adv Colloid Interface Sci.* 137 (2008) 57–81.
590 <https://doi.org/10.1016/j.cis.2007.07.007>.

- 591 [35] J. Kim, L.J. Cote, F. Kim, W. Yuan, K.R. Shull, J. Huang, Graphene oxide sheets at
592 interfaces, *J. Am. Chem. Soc.* 132 (2010) 8180–8186.
593 <https://doi.org/10.1021/ja102777p>.
- 594 [36] A.P. Kotula, S.L. Anna, Probing timescales for colloidal particle adsorption using slug
595 bubbles in rectangular microchannels, *Soft Matter*. 8 (2012) 10759–10772.
596 <https://doi.org/10.1039/C2SM25970B>.
- 597 [37] A.J. Morse, S.-Y. Tan, E.C. Giakoumatos, G.B. Webber, S.P. Armes, S. Ata, E.J.
598 Wanless, Arrested coalescence behaviour of giant Pickering droplets and colloidosomes
599 stabilised by poly(tert-butylaminoethyl methacrylate) latexes, *Soft Matter*. 10 (2014)
600 5669–5681. <https://doi.org/10.1039/C4SM00801D>.
- 601 [38] Y. Lin, A. Böker, H. Skaff, D. Cookson, A.D. Dinsmore, T. Emrick, T.P. Russell,
602 Nanoparticle Assembly at Fluid Interfaces: Structure and Dynamics, *Langmuir*. 21
603 (2005) 191–194. <https://doi.org/10.1021/la048000q>.
- 604 [39] L. Dai, R. Sharma, C.Y. Wu, Self-assembled structure of nanoparticles at a liquid-liquid
605 interface, *Langmuir : The ACS Journal of Surfaces and Colloids*. 21 (2005) 2641–2643.
606 <https://doi.org/10.1021/la047256t>.
- 607 [40] S. Cauvin, P.J. Colver, S.A.F. Bon, Pickering Stabilized Miniemulsion Polymerization:
608 Preparation of Clay Armored Latexes, *Macromolecules*. 38 (2005) 7887–7889.
609 <https://doi.org/10.1021/ma051070z>.
- 610 [41] N.J. Alvarez, S.L. Anna, T. Saigal, R.D. Tilton, L.M. Walker, Interfacial dynamics and
611 rheology of polymer-grafted nanoparticles at air-water and xylene-water interfaces,
612 *Langmuir*. 28 (2012) 8052–8063. <https://doi.org/10.1021/la300737p>.
- 613 [42] L. Isa, D.C.E. Calzolari, D. Pontoni, T. Gillich, A. Nelson, R. Zirbs, A. Sánchez-Ferrer,
614 R. Mezzenga, E. Reimhult, Core-shell nanoparticle monolayers at planar liquid-liquid
615 interfaces: effects of polymer architecture on the interface microstructure, *Soft Matter*. 9
616 (2013) 3789–3797. <https://doi.org/10.1039/C3SM27367A>.
- 617 [43] L. Isa, E. Amstad, K. Schwenke, E.D. Gado, P. Ilg, M. Kröger, E. Reimhult, Adsorption
618 of core-shell nanoparticles at liquid-liquid interfaces, *Soft Matter*. 7 (2011) 7663–7675.
619 <https://doi.org/10.1039/C1SM05407D>.
- 620 [44] M.S. Manga, T.N. Hunter, O.J. Cayre, D.W. York, M.D. Reichert, S.L. Anna, L.M.
621 Walker, R.A. Williams, S.R. Biggs, Measurements of Submicron Particle Adsorption
622 and Particle Film Elasticity at Oil-Water Interfaces, *Langmuir*. 32 (2016) 4125–4133.
623 <https://doi.org/10.1021/acs.langmuir.5b04586>.
- 624 [45] H. Fessi, F. Puisieux, J.Ph. Devissaguet, N. Ammoury, S. Benita, Nanocapsule
625 formation by interfacial polymer deposition following solvent displacement,
626 *International Journal of Pharmaceutics*. 55 (1989) R1–R4. [https://doi.org/10.1016/0378-5173\(89\)90281-0](https://doi.org/10.1016/0378-5173(89)90281-0).
- 628 [46] D. Arla, L. Flesinski, P. Bouriat, C. Dicharry, Influence of Alkaline pH on the Rheology
629 of Water/Acidic Crude Oil Interface, *Energy Fuels*. 25 (2011) 1118–1126.
630 <https://doi.org/10.1021/ef1015022>.
- 631 [47] P. Bouriat, N. El Kerri, A. Graciaa, J. Lachaise, Properties of a two-dimensional
632 asphaltene network at the water-cyclohexane interface deduced from dynamic
633 tensiometry, *Langmuir*. 20 (2004) 7459–7464. <https://doi.org/10.1021/la049017b>.
- 634 [48] C. Dicharry, D. Arla, A. Siquin, A. Graciaa, P. Bouriat, Stability of water/crude oil
635 emulsions based on interfacial dilatational rheology, *J Colloid Interface Sci*. 297 (2006)
636 785–791. <https://doi.org/10.1016/j.jcis.2005.10.069>.
- 637 [49] D. Jack, *Handbook of Clinical Pharmacokinetic Data* | David B. Jack | Palgrave
638 Macmillan, (1992). <https://www.palgrave.com/br/book/9781349224975> (accessed
639 February 1, 2019).

- 640 [50] M.R.C. Marques, R. Loebenberg, M. Almukainzi, Simulated biological fluids with
641 possible application in dissolution testing, *Dissolution Technologies*. 18 (2011) 15–28.
642 <https://doi.org/10.14227/DT180311P15>.
- 643 [51] N. Tsapis, Imaging Polymer Nanoparticles by Means of Transmission and Scanning
644 Electron Microscopy Techniques, in: C. Vauthier, G. Ponchel (Eds.), *Polymer*
645 *Nanoparticles for Nanomedicines*, Springer International Publishing, Cham, 2016: pp.
646 205–219. https://doi.org/10.1007/978-3-319-41421-8_8.
- 647 [52] B.P. Binks, T.S. Horozov, Aqueous foams stabilized solely by silica nanoparticles,
648 *Angew. Chem. Int. Ed. Engl.* 44 (2005) 3722–3725.
649 <https://doi.org/10.1002/anie.200462470>.
- 650 [53] K.L. Thompson, N. Cinotti, E.R. Jones, C.J. Mable, P.W. Fowler, S.P. Armes, Bespoke
651 Diblock Copolymer Nanoparticles Enable the Production of Relatively Stable Oil-in-
652 Water Pickering Nanoemulsions, *Langmuir*. 33 (2017) 12616–12623.
653 <https://doi.org/10.1021/acs.langmuir.7b02267>.
- 654 [54] S.M. Dieng, N. Anton, P. Bouriart, O. Thioune, N. Massaddeq, M. Diarra, T.
655 Vandamme, Pickering nano-emulsions stabilized by solid lipid nanoparticles as a
656 temperature sensitive drug delivery system, *Soft Matter*. (2019).
657 <https://doi.org/10.1039/C9SM01283D>.
- 658 [55] P.M. Sy, N. Anton, Y. Idoux-Gillet, S.M. Dieng, N. Messaddeq, S. Ennahar, M. Diarra,
659 T.F. Vandamme, Pickering nano-emulsion as a nanocarrier for pH-triggered drug
660 release, *International Journal of Pharmaceutics*. 549 (2018) 299–305.
661 <https://doi.org/10.1016/j.ijpharm.2018.07.066>.
- 662 [56] M.J. Rymaruk, K.L. Thompson, M.J. Derry, N.J. Warren, L.P.D. Ratcliffe, C.N.
663 Williams, S.L. Brown, S.P. Armes, Bespoke contrast-matched diblock copolymer
664 nanoparticles enable the rational design of highly transparent Pickering double
665 emulsions, *Nanoscale*. 8 (2016) 14497–14506. <https://doi.org/10.1039/C6NR03856E>.
- 666 [57] B. Binks, Binks, B. P. Particles as surfactants-similarities and differences. *Curr. Opin.*
667 *Colloid Interface Sci.* 7, 21-41, *Current Opinion in Colloid & Interface Science*. 7
668 (2002) 21–41. [https://doi.org/10.1016/S1359-0294\(02\)00008-0](https://doi.org/10.1016/S1359-0294(02)00008-0).
- 669 [58] J. Lucassen, M. Van Den Tempel, Dynamic measurements of dilational properties of a
670 liquid interface, *Chemical Engineering Science*. 27 (1972) 1283–1291.
671 [https://doi.org/10.1016/0009-2509\(72\)80104-0](https://doi.org/10.1016/0009-2509(72)80104-0).
- 672 [59] J. Lucassen, M. Van Den Tempel, Longitudinal waves on visco-elastic surfaces, *Journal*
673 *of Colloid and Interface Science*. 41 (1972) 491–498. [https://doi.org/10.1016/0021-](https://doi.org/10.1016/0021-9797(72)90373-6)
674 [9797\(72\)90373-6](https://doi.org/10.1016/0021-9797(72)90373-6).
- 675 [60] I. Velásquez, N. Anton, J. Sykora, J.C. Pereira, Tuning of properties of alkyl phenol
676 formaldehyde resins in petroleum demulsifiers. 2. Interfacial dilatational properties,
677 *Petroleum Science and Technology*. 35 (2017) 1124–1129.
678 <https://doi.org/10.1080/10916466.2017.1310883>.
- 679 [61] M. Tubic-Grozdanic, M.B. Bolger, P. Langguth, Application of Gastrointestinal
680 Simulation for Extensions for Biowaivers of Highly Permeable Compounds, *AAPS J.*
681 10 (2008) 213–226. <https://doi.org/10.1208/s12248-008-9023-x>.
- 682 [62] M. Yazdanian, K. Briggs, C. Jankovsky, A. Hawi, The “high solubility” definition of
683 the current FDA Guidance on Biopharmaceutical Classification System may be too
684 strict for acidic drugs, *Pharm. Res.* 21 (2004) 293–299.
685 <https://doi.org/10.1023/b:pham.0000016242.48642.71>.
- 686 [63] J.J. Sheng, N.A. Kasim, R. Chandrasekharan, G.L. Amidon, Solubilization and
687 dissolution of insoluble weak acid, ketoprofen: effects of pH combined with surfactant,
688 *Eur J Pharm Sci.* 29 (2006) 306–314. <https://doi.org/10.1016/j.ejps.2006.06.006>.

- 689 [64] R.-X. Bai, L.-H. Xue, R.-K. Dou, S.-X. Meng, C.-Y. Xie, Q. Zhang, T. Guo, T. Meng,
690 Light-Triggered Release from Pickering Emulsions Stabilized by TiO₂ Nanoparticles
691 with Tailored Wettability, *Langmuir*. 32 (2016) 9254–9264.
692 <https://doi.org/10.1021/acs.langmuir.6b02329>.
- 693 [65] W. Wang, A.H. Milani, Z. Cui, M. Zhu, B.R. Saunders, Pickering Emulsions Stabilized
694 by pH-Responsive Microgels and Their Scalable Transformation to Robust
695 Submicrometer Colloidosomes with Selective Permeability, *Langmuir*. 33 (2017)
696 8192–8200. <https://doi.org/10.1021/acs.langmuir.7b01618>.

697

698

699

700

701

702

703

